

# Cyclic Bending Failure of Local Sharp-Notched Circular Tubes with Different Diameter-to-Thickness Ratios

**Kuo-Long Lee\***

Professor, Dept. of Innovative Design and Entrepreneurship  
Management, Far East University, Tainan, Taiwan.  
\*email id: lk1@cc.feu.edu.tw

**Wen-Fung Pan**

Professor, Dept. of Engineering Science National Cheng Kung  
University, Tainan, Taiwan .  
email id: z7808034@email.ncku.edu.tw

\*Corresponding author

Date of publication (dd/mm/yyyy): 11/05/2018

**Abstract** – In this study, the failure of local sharp-notched 6061-T6 aluminum alloy tubes with different diameter-to-thickness ratios submitted to cyclic bending are studied. Different diameter-to-thickness ratios of 16.5, 31.0 and 60.0 were considered. The notch depths of tubes were considered from very small to about 0.6 times the tube's wall thickness. From the experimental moment-curvature relationship, it demonstrated a steady loop from the beginning of the first bending cycle. From the experimental ovalization-curvature relationship, it exhibited an increasing and ratcheting manner along with the number of bending cycles. The larger notch depth led to more asymmetrical ovalization-curvature relationship and the greater increase of the ovalization. Furthermore, for a certain diameter-to-thickness ratio, five unparallel straight lines corresponding to five different notch depths were found for the controlled curvature-number of cycles required to ignite failure relationship on a log-log scale. Finally, a theoretical model was proposed for simulating the aforementioned relationship. Through comparison with the experimental data, the model can properly simulate the experimental findings.

**Keywords** – Different Diameter-to-thickness Ratios, Local Sharp-notched 6061-T6 Aluminum Alloy Tubes, Cyclic Bending, Number of Cycles Required to Ignite Failure.

## I. INTRODUCTION

It is well known that bending of a circular tube results in ovalization (change in the outer diameter divided by the original outer diameter) of the tube's cross section. This ovalization increases slowly during reverse bending and subsequent cyclic bending, and in turn, results in the degradation of the circular tube, which buckles or fractures. When the ovalization reaches a critical value. Circular tubes are severely damaged during buckling and fracturing and cannot bear the load, which ultimately results in obstruction and leakage of the material being transported. As such, a complete understanding of the degradation and failure of circular tubes subjected to cyclic bending is essential for industrial applications.

In 1985, Prof. Kyriakides and his research team designed a bending machine and began a series of experimental and theoretical studies on tubes submitted to monotonic or cyclic bending with or without external or internal pressure. Kyriakides and Shaw [1] then extended the aforementioned research to evaluate the buckling failure of tubes under cyclic bending. Corona and Kyriakides [2] experimentally investigated the behavior of tubes subjected to cyclic bending with external pressure. Vaze and Corona [3] employed a similar bending machine to examine the

deterioration and collapse of square steel tubes submitted to cyclic bending. Moreover, Corona and Kyriakides [4] studied the tube's buckling under bending with external pressure. Corona, Lee and Kyriakides [5] investigated the anisotropy of the plastic deformation for tubes submitted to bending. Limam, Lee, Corana and Kyriakides [6] experimentally and theoretically discussed the inelastic collapse of tubes subjected to bending with internal pressure. Limam, Lee and Kyriakides [7] also examined the response and collapse of local-dented tubes undertaking pure bending with some internal pressure. Bechle and Kyriakides [8] experimentally investigated the localization of NiTi tubes submitted to bending. Jiang, Kyriakides, Bechle and Landis [9] studied the pseudoelastic response of NiTi tubes subjected to bending.

In 1998, Pan, Wang and Hsu [10] designed and set up a new measurement apparatus. The apparatus was used with a cyclic bending machine to study various types of tube under different cyclic bending conditions. For examples: Pan and Fan [11] studied the effect of the prior curvature-rate at the preloading stage on subsequent creep or relaxation behavior, and Chang and Pan [12] discussed the buckling life estimation of circular tubes subjected to cyclic bending.

In 2010, the research team of Prof. Pan began to experimentally and theoretically investigate the response and the collapse of sharp-notched circular tubes submitted to cyclic bending. Lee, Hung and Pan [13] experimentally studied the relationship between the variation of ovalization and the number of bending cycles for sharp-notched circular tubes subjected to cyclic bending. Lee [14] then later investigated the response of sharp-notched SUS304 stainless steel tubes under cyclic bending, and found the asymmetrical, ratcheting, and increasing trends of ovalization-curvature relationships. In addition, Lee, Hsu and Pan [15] evaluated the viscoplastic response and buckling of sharp-notched SUS304 stainless steel circular tubes undertaking cyclic bending. Both the different notch depths and curvature rates were examined. Lee, Hsu and Pan [16] studied the response of sharp-notched circular tubes under pure bending creep and pure bending relaxation. Chung, Lee and Pan [17] investigated the collapse of sharp-notched 6061-T6 aluminum alloy tubes subjected to cyclic bending. However, the sharp notch for the aforementioned investigations was a circumferential sharp notch as shown in Fig. 1.

The investigation of the influence of the  $D_o/t$  ratio on the response and failure was first investigated by Lee, Pan and Kuo [18]. The 304 stainless steel smooth tubes with four

different  $D_o/t$  ratios of 30, 40, 50 and 60 were tested under cyclic bending. Later, Chang, Lee and Pan [19] studied the buckling failure of 301 stainless steel smooth tubes with different  $D_o/t$  ratios subjected to cyclic bending. In 2012, Lee, Hsu and Pan [20] started to investigate the influence of the  $D_o/t$  ratio on the response and failure of sharp-notched 304 stainless tubes subjected to cyclic bending. The type of the sharp notch was in Fig. 1 and three different  $D_o/t$  ratios were 16.25, 21.20 and 24.46. They discovered that five almost parallel straight lines corresponding to five different notch depths for each  $D_o/t$  ratio were observed from the relationship between the controlled curvature and number of bending cycles required to produce failure on a log-log scale. In addition, the slopes for the aforementioned relationship for three different  $D_o/t$  ratios were almost the same.

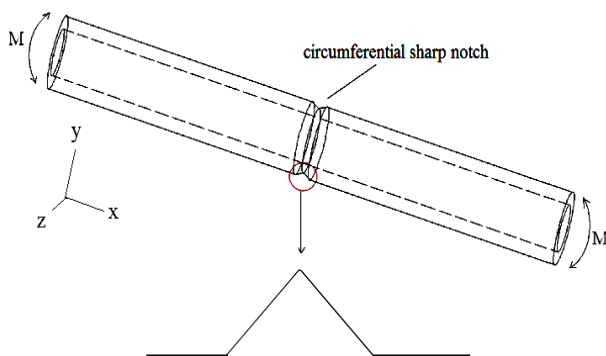


Fig. 1. A schematic drawing of the circumferential sharp-notched circular tube.

In this paper, local sharp-notched 6061-T6 aluminum alloy tubes with different  $D_o/t$  ratios of 16.5, 31.0 and 60.0 submitted to cyclic bending were experimentally studied. Related experimental tests were conducted by using the tube-bending machine and curvature-ovalization measurement apparatus. The quantities of the moment, curvature and ovalization were measured by sensors on testing facilities. Additionally, the number of cycles required to ignite failure was also recorded.

## II. EXPERIMENT

A tube-bending machine and a curvature-ovalization measurement apparatus were used to conduct the cyclic bending test on local sharp-notched 6061-T6 aluminum alloy tubes with different  $D_o/t$  ratios. The details on the experimental device, materials, specimens, and test procedures were presented in the sections that follow.

### A. Experimental Device

Fig. 2 schematically shows the experiments executed by a specially built tube-bending machine. This facility was built to conduct monotonic, reverse, and cyclic bending tests. A detailed explanation of the experimental facility can be found in many papers (Pan, Wang and Hsu [10], Pan and Fan [11]). Pan, Wang and Hsu [10] designed a new light-weight apparatus to measure the curvature and the ovalization of the tube's cross section shown in Fig. 3. Two side-inclinometers in the apparatus were used to detect the

tube's angle variation during cyclic bending. The tube curvature can be determined by a simple calculation according to the angle changes. An extended version of the calculation can be found in the work by Pan *et al.* [10]. In addition, the tube ovalization can be measured in the center part of the apparatus that included a magnetic detector and a magnetic block.

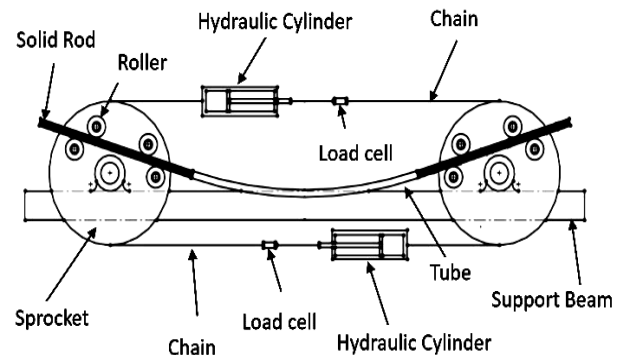


Fig. 2. A schematic drawing of the bending device.

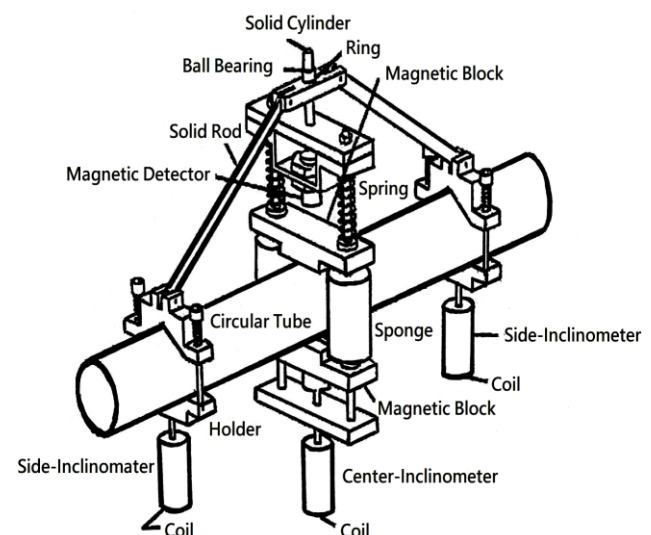


Fig. 3. A schematic drawing of the curvature-ovalization measurement apparatus.

### B. Material and Specimen

Circular tubes made of 6061-T6 aluminum alloy were adopted in this study. Table 1 shows the alloy's chemical composition in weight percentage. The ultimate stress is 258 MPa, the 0.2% strain offsetting yield stress is 166 MPa, and the percent elongation is 23%.

Table 1 - Chemical composition of 6061-T6 aluminum alloy (weight %).

Chemical Composition	Al	Mg	Si	Ti	Fe
Proportion (%)	98.096	0.937	0.535	0.012	0.139
Chemical Composition	Mn	Zn	Cr	Ni	
Proportion (%)	0.022	0.0983	0.022	0.005	

The raw, smooth 6061-T6 aluminum alloy circular tubes had a length  $L_0$  of 800 mm, an outer diameter  $D_o$  of 35.0 mm and a wall thickness  $t$  of 3.0 mm. The raw tubes were machined on the outside surface to obtain the desired  $D_o/t$  ratios of 16.5, 31.0 and 60.0 as shown in Fig. 4. Next, tubes with a certain  $D_o/t$  ratio were processed on the outside surface again to obtain the desired shape and depth of the notch ( $a$ ). In this study, five different depth-to-thickness ( $a/t$ ) ratios were considered: 0.0, 0.15, 0.3, 0.45, and 0.6. Note that  $a/t = 0.0$  represents a tube with a smooth surface. It can be seen from Fig. 4 that the magnitudes of  $t$  for  $D_o/t$  ratios of 16.5, 31.0 and 60.0 are 2.0, 1.0 and 0.5 mm, respectively. Therefore, the magnitudes of  $a$  for  $D_o/t = 16.5$  are 0.0, 0.3, 0.6, 0.9 and 1.2 mm. The magnitudes of  $a$  for  $D_o/t = 31.0$  are 0.0, 0.15, 0.3, 0.45, and 0.6 mm and the magnitudes of  $a$  for  $D_o/t = 60.0$  are 0.0, 0.075, 0.15, 0.225, and 0.3 mm. Fig. 5 shows a schematic drawing of a local sharp-notched circular tube.

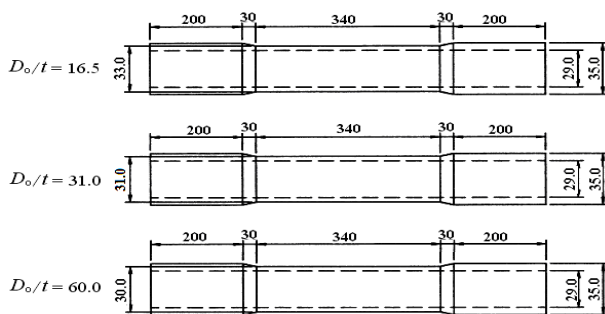


Fig. 4. A Schematic drawing of tube's dimensions for  $D_o/t$  ratios of 16.5, 31.0 and 60.0.

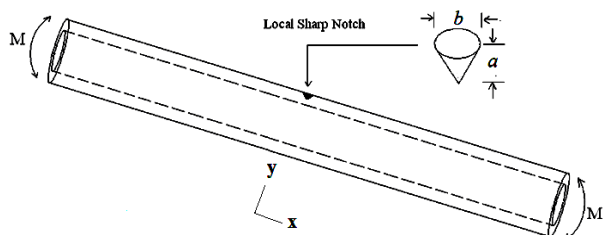


Fig. 5. A schematic drawing of a tube with a local sharp-notched depth of  $a$ .

### C. Test Procedures

The test involved a curvature-controlled cyclic bending. The controlled-curvature ranges were from  $\pm 0.2$  to  $\pm 1.1 \text{ m}^{-1}$ , and the curvature rate of the cyclic bending test was  $0.035 \text{ m}^{-1}\text{s}^{-1}$ . The magnitude of the bending moment was measured by two load cells mounted to the bending device. The magnitude of the curvature and ovalization of the tube's cross section were controlled and measured by the curvature-ovalization measurement apparatus. In addition, the number of cycles required to ignite failure was recorded.

## III. EXPERIMENTAL RESULTS AND DISCUSSION

### A. Mechanical Response

Fig. 6 shows a typical set of experimentally determined cyclic moment ( $M$ ) - curvature ( $\kappa$ ) curves for a local sharp-notched 6061 - T6 aluminum alloy circular tube, with  $D_o/t$

= 16.5 and  $a = 1.2 \text{ mm}$ , subjected to cyclic bending. The tubes were cycled between  $\kappa = \pm 0.4 \text{ m}^{-1}$ . The  $M$ - $\kappa$  response was seen to be characterized by a nearly closed and steady hysteresis loop from the first bending cycle. Since the sharp notch is small and local, the notch depth has almost no influence on the  $M$ - $\kappa$  curve. Therefore, the  $M$ - $\kappa$  curves for  $D_o/t = 16.5$  and different  $a$  are not shown in this paper.

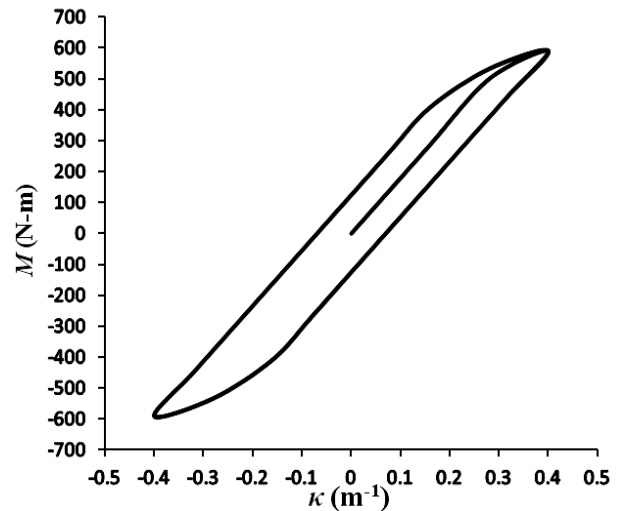


Fig. 6. Experimental moment ( $M$ ) - curvature ( $\kappa$ ) curve for a local sharp-notched 6061-T6 aluminum alloy tube with  $D_o/t = 16.5$  and  $a = 1.2 \text{ mm}$  under cyclic bending.

Figs. 7 and 8 demonstrate typical sets of experimentally determined cyclic moment ( $M$ ) - curvature ( $\kappa$ ) curves for local sharp-notched 6061-T6 aluminum alloy circular tubes, with  $D_o/t = 31.0$ ,  $a = 0.6 \text{ mm}$  and  $D_o/t = 60.0$ ,  $a = 0.3 \text{ mm}$ , respectively, subjected to cyclic bending. The tubes were cycled between  $\kappa = \pm 0.4 \text{ m}^{-1}$ . Similar phenomenon of the  $M$ - $\kappa$  curves with Fig. 6 was found. Because the thicknesses for  $D_o/t = 31.0$  and 60.0 are smaller, so the bending moments at the  $\kappa = + 0.4 \text{ m}^{-1}$  are smaller. Again, the sharp notch is small and local, the notch depth has almost no influence on the  $M$ - $\kappa$  curve. Therefore, the  $M$ - $\kappa$  curves for  $D_o/t = 31.0$  and 60.0 and different  $a$  are not shown in this paper.

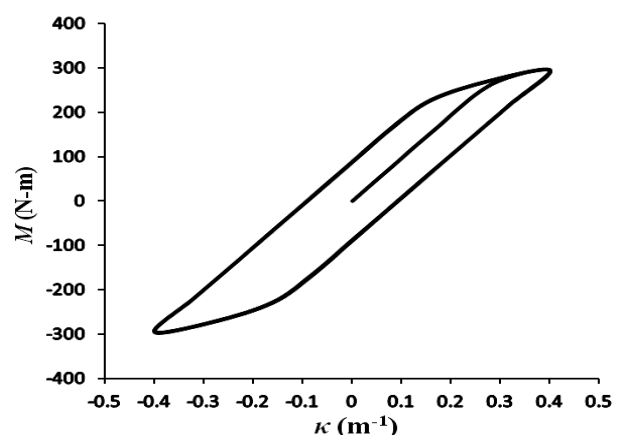


Fig. 7. Experimental moment ( $M$ ) - curvature ( $\kappa$ ) curve for a local sharp-notched 6061-T6 aluminum alloy tube with  $D_o/t = 31.0$  and  $a = 0.6 \text{ mm}$  under cyclic bending.

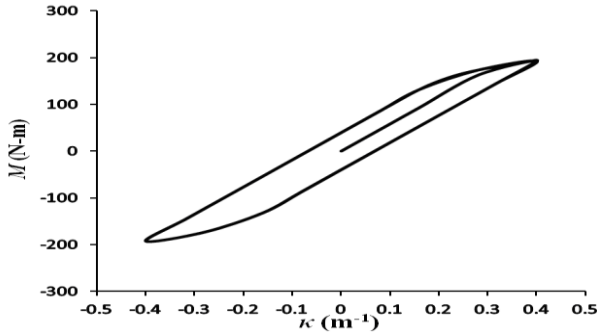


Fig. 8. Experimental moment ( $M$ ) - curvature ( $\kappa$ ) curve for a local sharp-notched 6061-T6 aluminum alloy tube with  $D_0/t = 60.0$  and  $a = 0.3$  mm under cyclic bending.

The experimental ovalization ( $\Delta D_0/D_0$ ) - curvature ( $\kappa$ ) relationships for local sharp-notched 6061-T6 aluminum alloy tubes with  $D_0/t = 16.5$  and  $a = 0.0, 0.3, 0.6, 0.9$ , and  $1.2$  mm subjected to cyclic bending are shown in Fig. 9(a)-Fig. 9(e), respectively. The tubes were cycled between  $\kappa = \pm 0.4 \text{ m}^{-1}$ . It is noted that the  $\Delta D_0/D_0$ - $\kappa$  curves exhibit a ratcheting trend and increase with the number of bending cycles. A larger  $a$  leads to a more asymmetrical look to the  $\Delta D_0/D_0$ - $\kappa$  curve. Moreover, a larger  $a$  leads to a larger ovalization.

The ovalization ( $\Delta D_0/D_0$ ) - curvature ( $\kappa$ ) relationships for local sharp-notched 6061-T6 aluminum alloy tubes with  $D_0/t = 31.0$  and  $a = 0.0, 0.15, 0.3, 0.45$ , and  $0.6$  mm subjected to cyclic bending are shown in Fig. 10(a)-Fig. 10(e), respectively. The ovalization ( $\Delta D_0/D_0$ ) - curvature ( $\kappa$ ) relationships for local sharp-notched 6061-T6 aluminum alloy tubes with  $D_0/t = 60.0$  and  $a = 0.0, 0.075, 0.15, 0.225$ , and  $0.3$  mm subjected to cyclic bending are shown in Fig. 11(a)-Fig. 11(e), respectively. The tubes were cycled between  $\kappa = \pm 0.4 \text{ m}^{-1}$ . It is demonstrated that

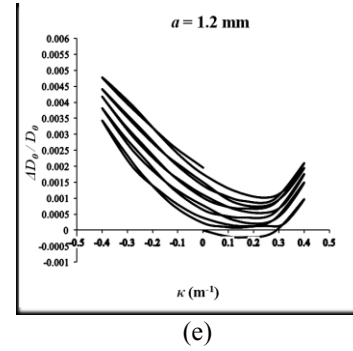


Fig. 9. Experimental ovalization ( $\Delta D_0/D_0$ ) - curvature ( $\kappa$ ) curves for local sharp-notched 6061-T6 aluminum alloy tubes with  $D_0/t = 16.5$  and  $a =$  (a)  $0.0$ , (b)  $0.3$ , (c)  $0.6$ , (d)  $0.9$  and (e)  $1.2$  mm subjected to cyclic bending.

The  $\Delta D_0/D_0$ - $\kappa$  curves also exhibit a ratcheting trend and increase with the number of bending cycles. A larger  $a$  also leads to a more asymmetrical appearance of the  $\Delta D_0/D_0$ - $\kappa$  curve and a larger ovalization. In addition, for a constant  $a$  of  $0.3$  mm in Fig. 9(b), Fig. 10(c) and Fig. 11(e), a larger  $D_0/t$  ratio leads to a larger ovalization.

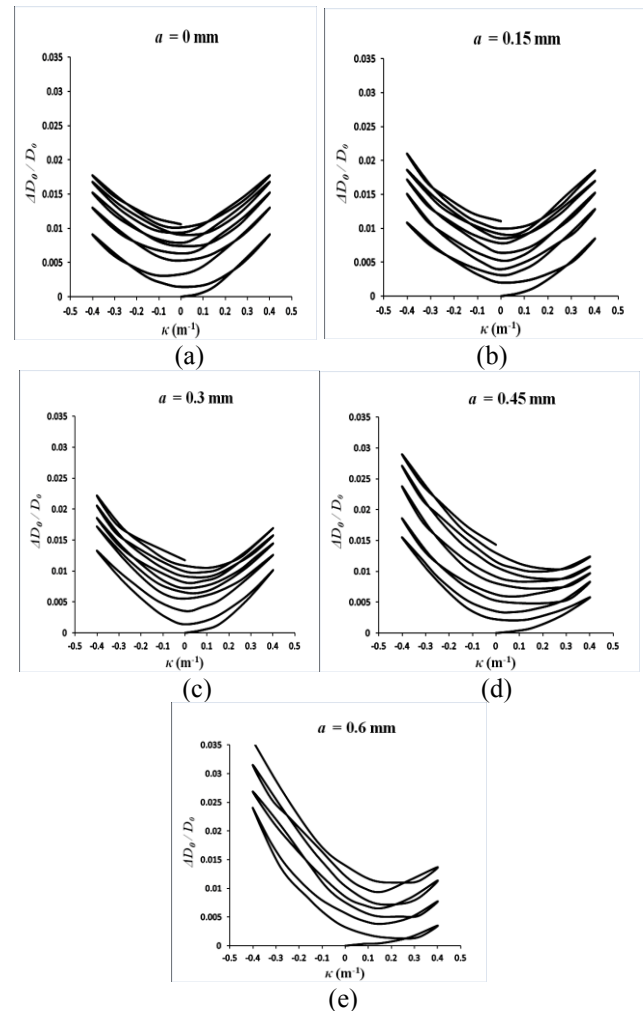
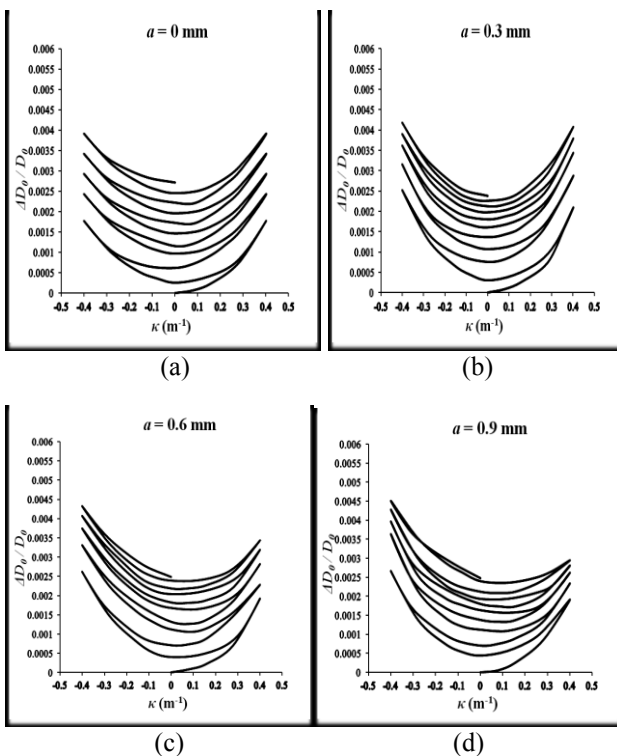


Fig. 10. Experimental ovalization ( $\Delta D_0/D_0$ ) - curvature ( $\kappa$ ) curves for local sharp-notched 6061-T6 aluminum alloy tubes with  $D_0/t = 31.0$  and  $a =$  (a)  $0.0$ , (b)  $0.15$ , (c)  $0.3$ , (d)  $0.45$  and (e)  $0.6$  mm subjected to cyclic bending.





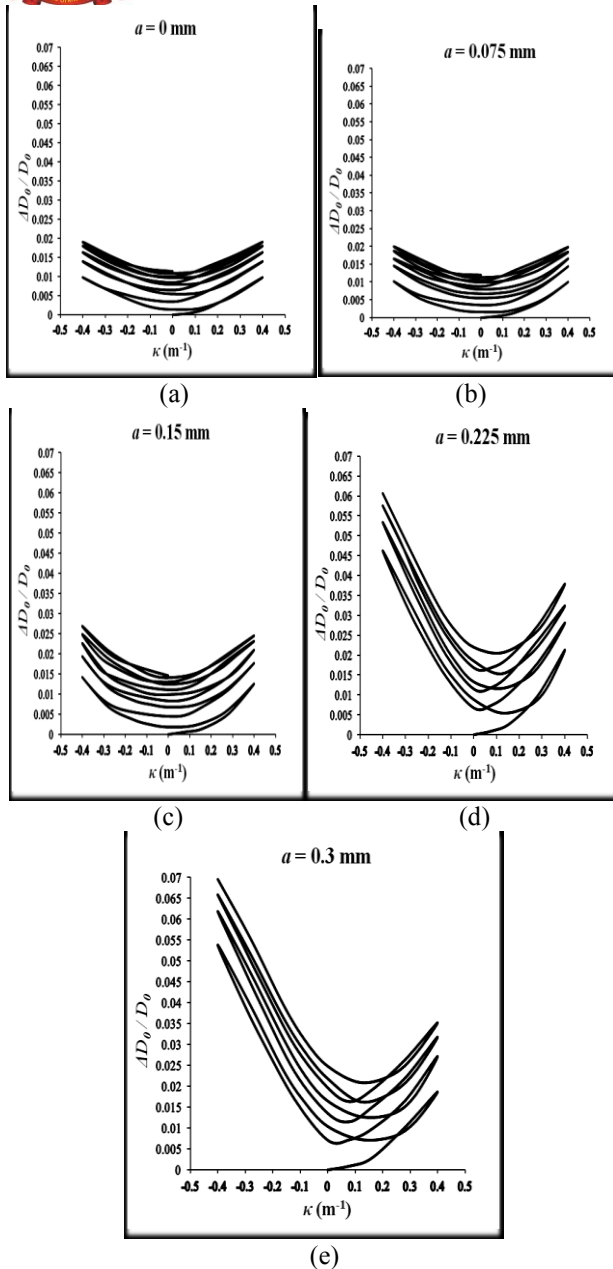


Fig.11. Experimental ovalization ( $\Delta D_0/D_0$ ) - curvature ( $\kappa$ ) curves for local sharp-notched 6061-T6 aluminum alloy tubes with  $D_0/t = 60.0$  and  $a =$  (a) 0.0, (b) 0.075, (c) 0.15, (d) 0.225 and (e) 0.3 mm subjected to cyclic bending.

### B. Failure

Fig. 12(a)-Fig. 12(c) present the experimental data of the cyclic controlled curvature ( $\kappa_c/\kappa_0$ ) versus the number of cycles required to ignite failure ( $N_f$ ) for local sharp-notched 6061-T6 aluminum alloy tubes with  $D_0/t = 16.5$ , 31.0 and 60.0, respectively, subjected to cyclic bending. The controlled curvature was normalized by  $\kappa_0 = t/D_0^2$  [2]. For a certain  $\kappa_c/\kappa_0$  and  $a$ , tubes with a larger  $D_0/t$  ratios led to a lower  $N_f$ . In addition, for a certain  $D_0/t$  ratio and  $\kappa_c/\kappa_0$ , tubes with a larger  $a$  led to a lower  $N_f$ .

Subsequently, the experimental data in Fig. 12(a)-Fig. 12(c) were plotted on a log-log scale, and five straight dot lines were observed in Fig. 13(a)-Fig. 13(c). Note that the dot lines were determined by the least square method. It can

be seen that five unparallelled dot lines corresponding to five different  $a$  for each  $D_0/t$  ratio.

In 1987, Kyriakides and Shaw [1] proposed an empirical formulation to describe the relationship between  $\kappa_c/\kappa_0$  and  $N_f$  to be:

$$\kappa_c/\kappa_0 = C (N_f)^{-\alpha} \quad (1)$$

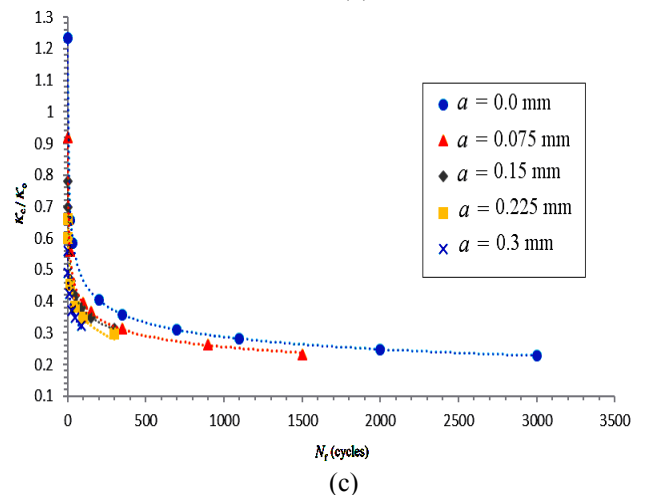
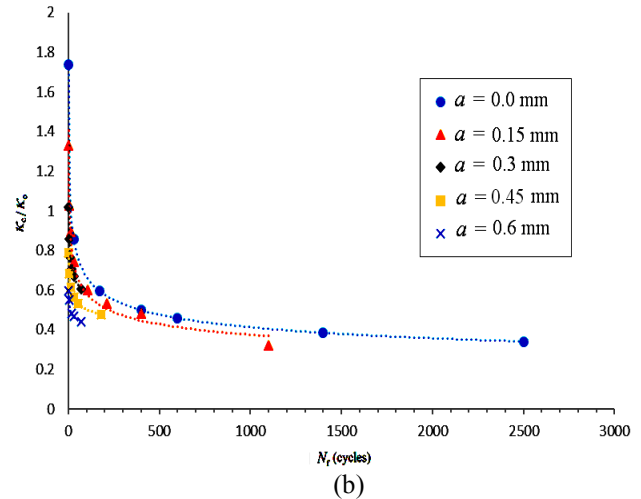
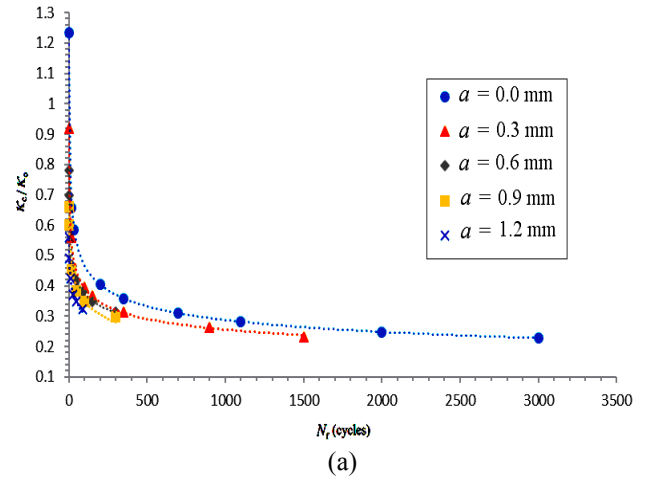


Fig.12. Experimental controlled curvature ( $\kappa_c/\kappa_0$ ) - number of cycles required to ignite failure ( $N_f$ ) curves for local sharp-notched 6061-T6 aluminum alloy tubes with  $D_0/t =$  (a) 16.5, (b) 31.0 and (c) 60.0 under cyclic bending.

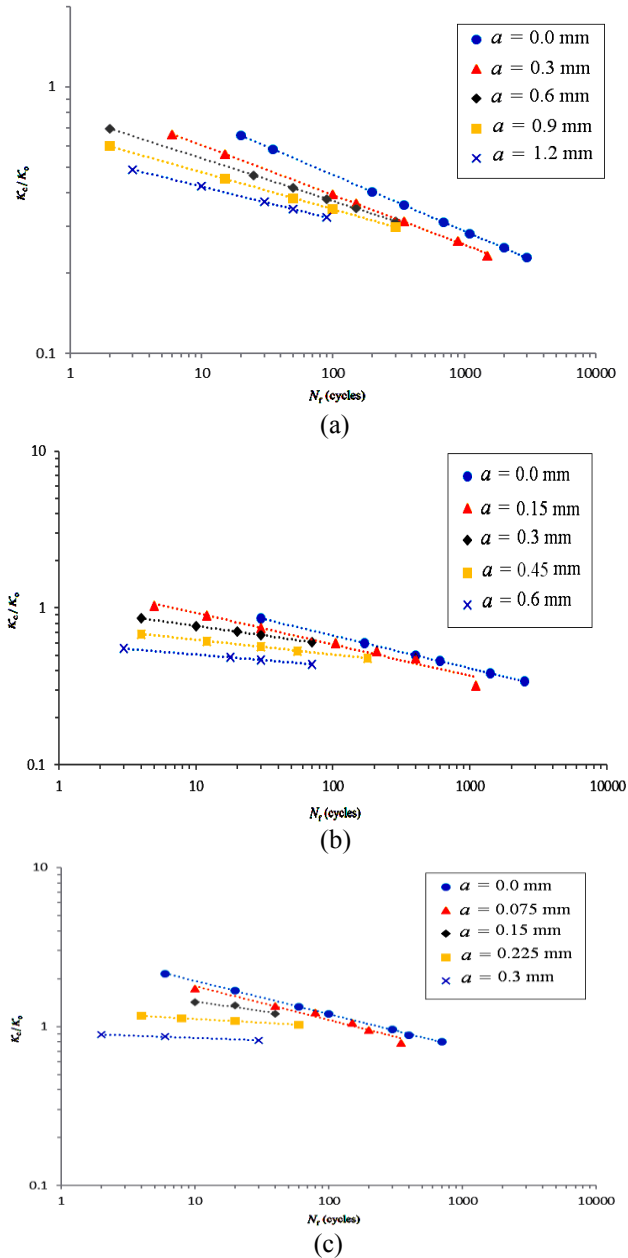


Fig.13. Experimental controlled curvature ( $\kappa_c/\kappa_0$ ) - number of cycles required to ignite failure ( $N_f$ ) curves for local sharp-notched 6061-T6 aluminum alloy tubes with  $D_o/t =$  (a) 16.5, (b) 31.0 and (c) 60.0 under cyclic bending on a log-log scale.

or

$$\log \kappa_c/\kappa_0 = \log C - \alpha \log N_f \quad (2)$$

where  $C$  and  $\alpha$  are the material parameters, which are related to the material and  $D_o/t$  ratios. The parameter  $C$  is the amount of  $\kappa_c/\kappa_0$  when  $N_f = 1$ , and the parameter  $\alpha$  is the slope of the log-log plot. The formulation has been successfully simulated the  $\kappa_c/\kappa_0$ - $N_f$  relationships for 6061-T6 aluminum alloy and 1018 carbon steel smooth tubes subjected to cyclic bending [1].

In this study, the liner relationships between  $\ln C$  and  $a/t$  and  $\ln \alpha$  and  $a/t$  were found in Fig. 14(a)-Fig. 14(c) and Fig. 15(a)-Fig. 15(c). Therefore, we write

$$\ln C = C_o - \beta (a/t) \quad (3)$$

and

$$\ln \alpha = \alpha_o - \gamma (a/t) \quad (4)$$

where  $C_o$ ,  $\beta$ ,  $\alpha_o$  and  $\gamma$  are material parameters. Due to the linear relationship, the quantities of  $C_o$  and  $\beta$  were the intercepts and slopes in Fig. 14(a)-Fig. 14(c) for  $D_o/t = 16.5$ , 31.0 and 60.0, respectively, and quantities of  $\alpha_o$  and  $\gamma$  were the intercepts and slopes in Fig. 15(a)-Fig. 15(c) for  $D_o/t = 16.5$ , 31.0 and 60.0, respectively.

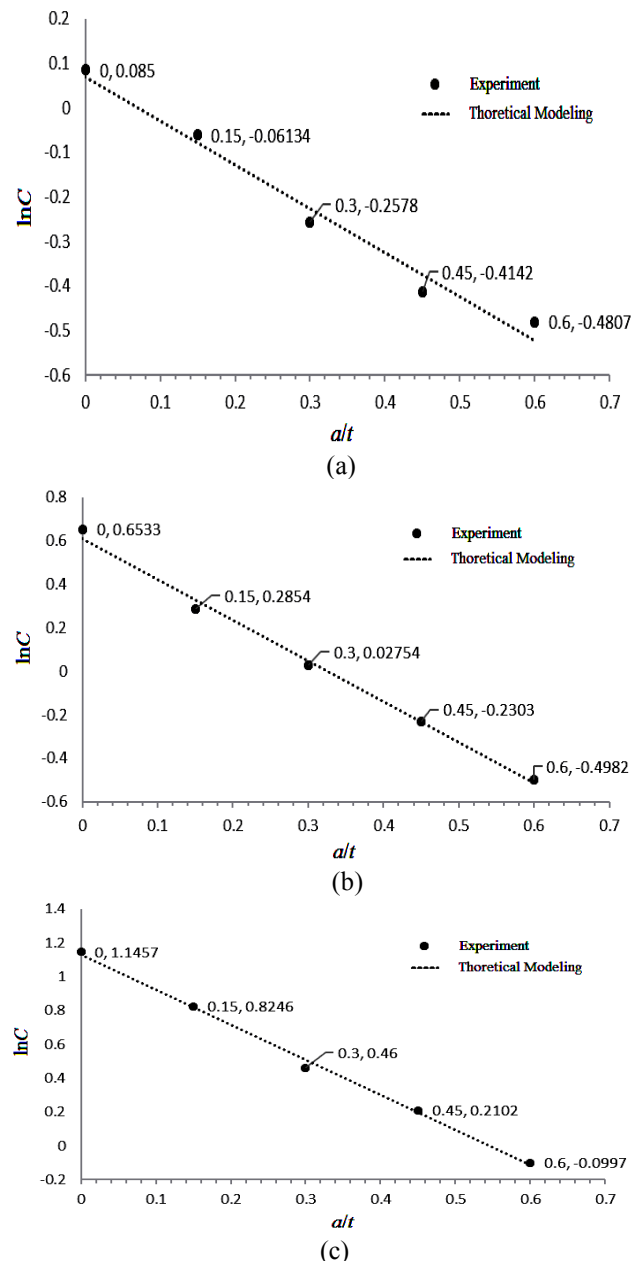


Fig.14. The relationship between  $\ln C$  and  $a/t$  for  $D_o/t =$  (a) 16.5, (b) 31.0 and (c) 60.

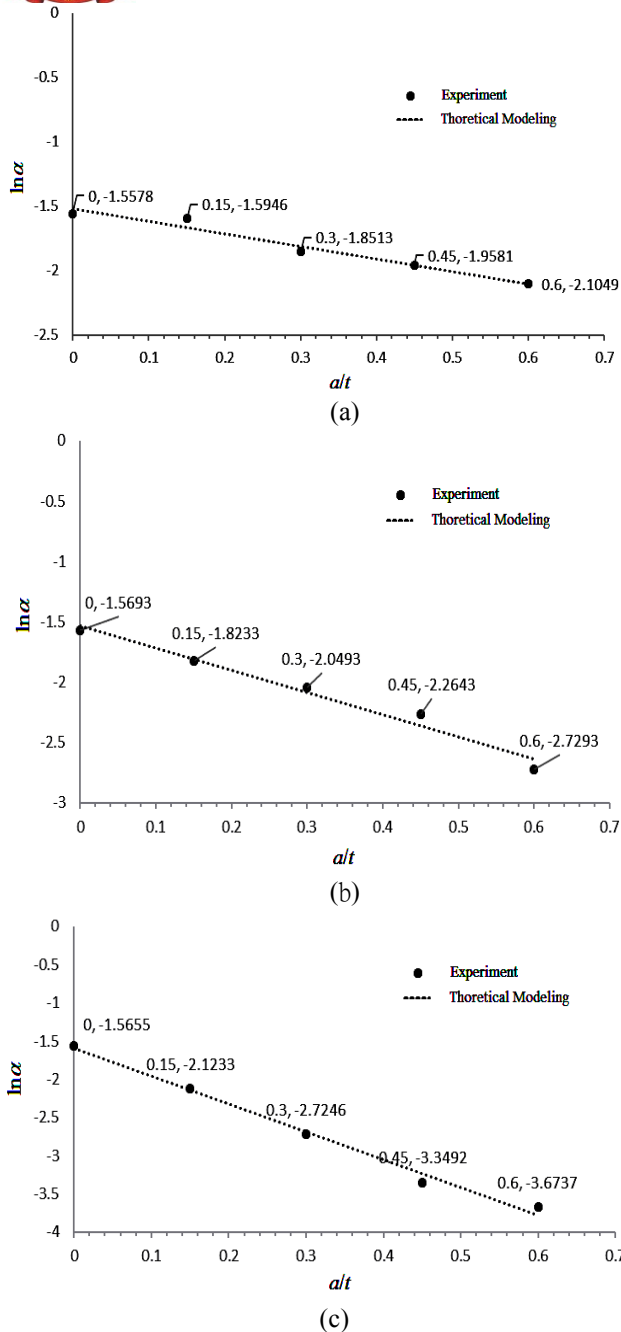


Fig. 15. The relationship between  $\ln \alpha$  and  $a/t$  for  $D_o/t =$  (a) 16.5, (b) 31.0 and (c) 60.0.

Next, we tried to find the linear relationships for material parameters  $C_o$ ,  $\beta$ ,  $\alpha_o$  and  $\gamma$  with the  $D_o/t$  ratios. After a lot of attempts, the linear relationships from Fig. 16(a)-Fig. 16(d) were written as:

$$C_o^2 = a_1(D_o/t) + a_2 \quad (5)$$

$$\beta^2(D_o/t) = b_1(D_o/t) + b_2 \quad (6)$$

$$\alpha_o^2(D_o/t) = c_1(D_o/t) + c_2 \quad (7)$$

and

$$1/\gamma = d_1/(D_o/t) + d_2 \quad (8)$$

where  $a_1$ ,  $a_2$ ,  $b_1$ ,  $b_2$ ,  $c_1$ ,  $c_2$ ,  $d_1$  and  $d_2$  are material constants. The values of  $a_1$ ,  $b_1$ ,  $c_1$  and  $d_1$  were the slope in Fig 16(a)-Fig. 16(d), respectively. The amounts of  $a_2$ ,  $b_2$ ,  $c_2$  and  $d_2$  were the intercept in Fig 16(a) - Fig. 16(d), respectively.

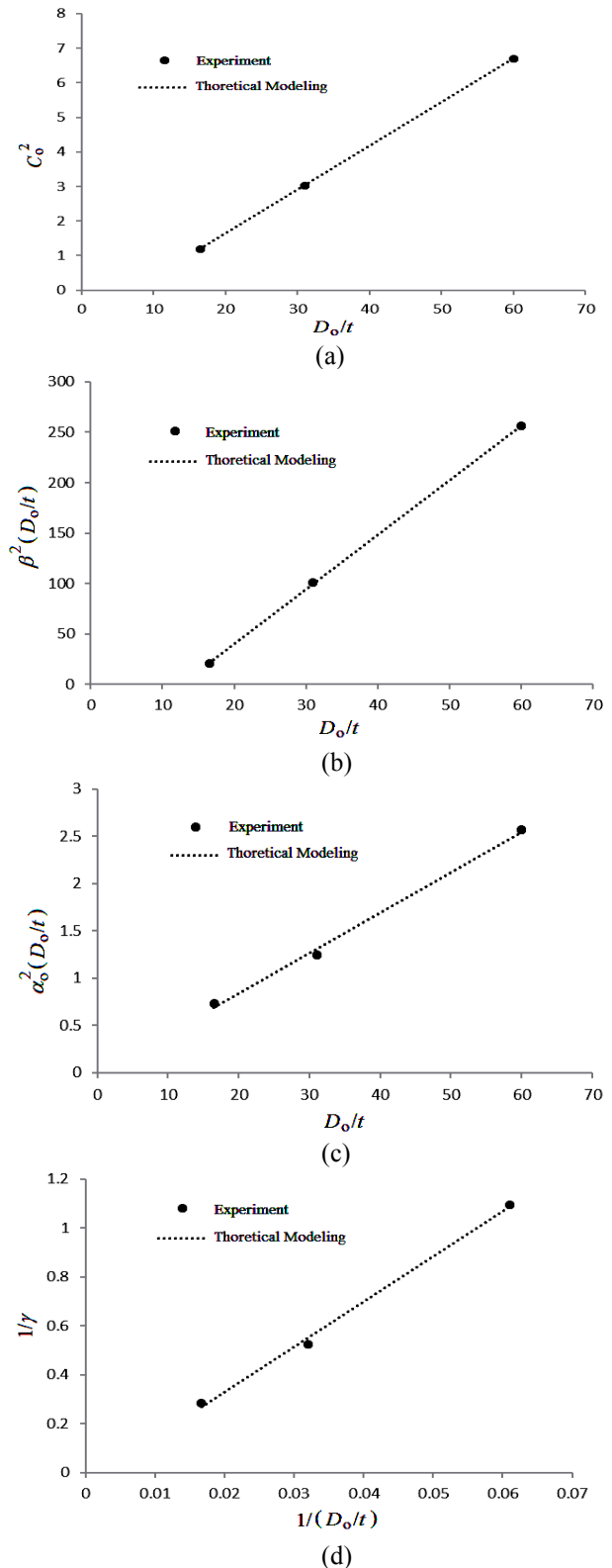


Fig. 16. (a) The relationship between  $C_o^2$  and  $D_o/t$ , (b) the relationship between  $\beta^2(D_o/t)$  and  $D_o/t$ , (c) the relationship between  $\alpha_o^2(D_o/t)$  and  $D_o/t$ , and (d) the relationship between  $1/\gamma$  and  $1/(D_o/t)$ .

Finally, Eq. (2)-Eq. (8) and the material parameters had been obtained were used to simulate the experimental data in Fig. 13(a)-Fig. 13(c). The simulated results of the relationship between the controlled curvature ( $\kappa_c/\kappa_0$ ) and number of cycles required to ignite failure ( $N_f$ ) curves for local sharp-notched 6061-T6 aluminum alloy tubes with  $D_o/t = 16.5, 31.0$  and  $60.0$ , respectively, under cyclic bending on a log-log scale are depict in Fig. 17(a)- Fig. 17(c) in solid lines. Good agreement between the experimental and simulated results has been achieved

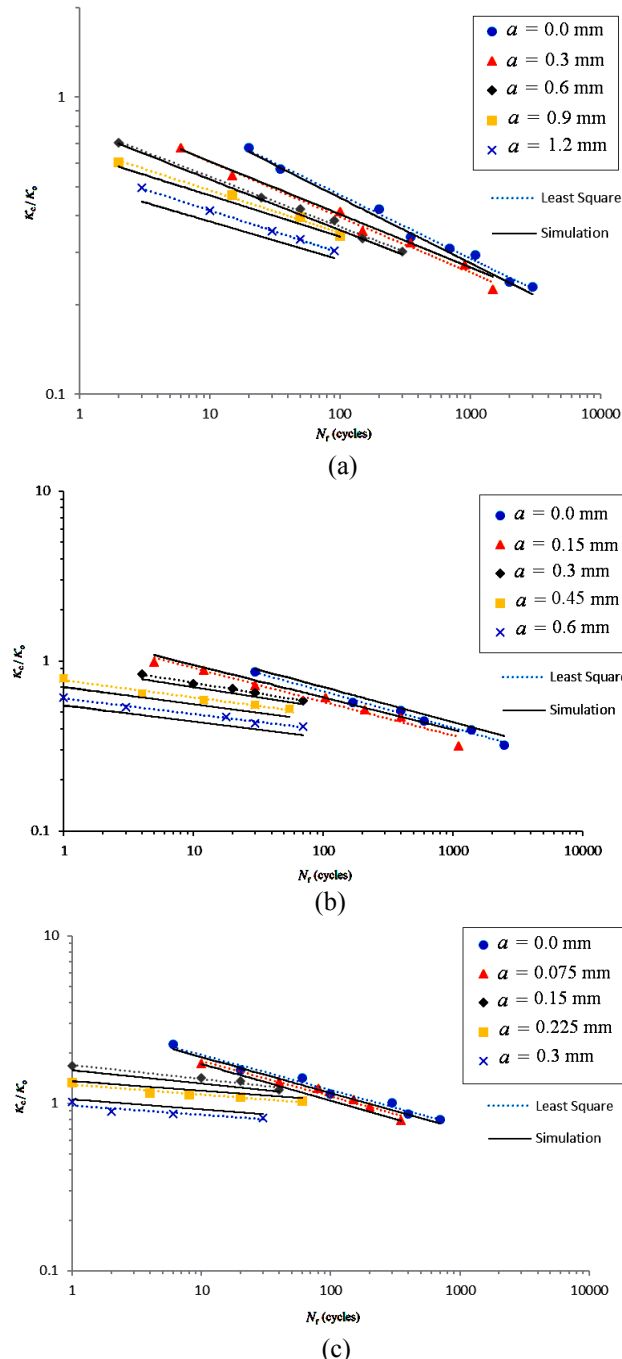


Fig. 17. Experimental and simulated controlled curvature ( $\kappa_c/\kappa_0$ ) - number of cycles required to ignite failure ( $N_f$ ) curves for local sharp-notched 6061-T6 aluminum alloy tubes with  $D_o/t =$  (a) 16.5, (b) 31.0 and (c) 60.0 under cyclic bending on a log-log scale.

## IV. CONCLUSIONS

This study investigated the response and failure of the local sharp-notched 6061-T6 aluminum alloy tubes with different  $D_o/t$  ratios submitted to cyclic bending. Some important conclusions are sorted as follows according to the experimental and simulated results:

- 1) The experimental  $M-\kappa$  relationship for the local sharp-notched 6061-T6 aluminum alloy tubes with any  $a$  or  $D_o/t$  ratio displayed a closed hysteresis loop from the first bending cycle. Since the sharp notch was small and local, the notch depth had almost no influence on the  $M-\kappa$  curve for a certain  $D_o/t$  ratio.
- 2) The experimental  $\Delta D_o/D_o-\kappa$  relationship for local sharp-notched 6061-T6 aluminum alloy tubes with any  $D_o/t$  ratio or  $a$  revealed an increasing and ratcheting trend with the number of bending cycles. The  $\Delta D_o/D_o-\kappa$  relationships were symmetrical for  $a = 0.0$  mm, but asymmetrical for  $a \neq 0.0$  mm. In addition, the tubes with a larger  $D_o/t$  or  $a$  led to more asymmetrical trend and a larger ovalization.
- 3) The empirical formulation of Eq. (2) proposed by Kyriakides and Shaw [1] was modified to simulate the  $\kappa/\kappa_0-N_f$  relationship for the local sharp-notched 6061-T6 aluminum alloy tubes with different  $D_o/t$  ratios submitted to cyclic bending. According to the experimental data, the forms of the material parameters,  $C$  and  $\alpha$ , were proposed in Eq. (3) and Eq. (4), respectively. In addition, The forms of the material parameters,  $C_0$ ,  $\beta$ ,  $\alpha_0$  and  $\gamma$ , were proposed in Eq. (5)-Eq. (8), respectively. The results simulated by Eq. (2)-Eq. (8) were in good agreement with the experimental findings (Fig. 17(a)-Fig. 17(c)).

## ACKNOWLEDGMENT

The work presented was carried out with the support of the National Science Council under grant MOST 105-2221-E-006-073. Its support is gratefully acknowledged.

## REFERENCES

- [1] S. Kyriakides, and P.-K. Shaw, "Inelastic buckling of tubes under cyclic loads," *J. Pres. Ves. Tech.*, vol. 109, no. 2, 1987, pp. 169-178.
- [2] E. Corona, and S. Kyriakides, "An experimental investigation of the degradation and buckling of circular tubes under cyclic bending and external pressure," *Thin-Walled Struct.*, vol. 12, no. 3, 1991, pp. 229-263.
- [3] S. Vaze, and E. Corona, "Degradation and collapse of square tubes under cyclic bending," *Thin-Walled Struct.*, vol. 31, no. 4, 1998, pp. 325-341.
- [4] E. Corona, and S. Kyriakides, "Asymmetric collapse modes of pipes under combined bending and pressure," *Int. J. Solids Struct.*, vol. 24, no. 5, 2000, pp. 505-535.
- [5] E. Corona, L.-H. Lee, and S. Kyriakides, "Yield anisotropic effects on buckling of circular tubes under bending," *Int. J. Solids Struct.*, vol. 43, no. 22, 2006, pp. 7099-7118.
- [6] A. Limam, L.-H. Lee, E. Corona, and S. Kyriakides, "Inelastic wrinkling and collapse of tubes under combined bending and internal pressure," *Int. J. Mech. Sci.*, vol. 52, no. 5, 2010, pp. 37-47.
- [7] A. Limam, L.-H. Lee, and S. Kyriakides, "On the collapse of dented tubes under combined bending and internal pressure," *Int.*



- J. Solids Struct.*, vol. 55, no. 1, 2012, pp. 1-12.
- [8] N. J. Bechle, and S. Kyriakides, "Localization of NiTi tubes under bending," *Int. J. Solids Struct.*, vol. 51, no. 5, 2014, pp. 967-980.
  - [9] D. Jiang, S. Kyriakides, N. J. Bechle and C. M. Landis, "Bending of pseudoelastic NiTi tubes," *Int. J. Solids Struct.*, vol. 124, 2017, pp. 192-214.
  - [10] W.-F. Pan, T.-R. Wang, and C.-M. Hsu, "A curvature-ovalization measurement apparatus for circular tubes under cyclic bending," *Exp. Mech.*, vol. 38, no. 2, 1998, pp. 99-102.
  - [11] W.-F. Pan, and C.-H. Fan, "An experimental study on the effect of curvature-rate at preloading stage on subsequent creep or relaxation of thin-walled tubes under pure bending," *JSME Int. J., Ser. A*, vol. 41, no. 4, 1998, pp. 525 -531.
  - [12] K.-H. Chang, and W.-F. Pan, "Buckling life estimation of circular Tubes under Cyclic Bending," *Int. J. Solids Struct.*, vol. 46, no. 2, 2009, pp. 254-270.
  - [13] K.-L. Lee, C.-Y. Hung, and W.-F. Pan, "Variation of ovalization for sharp-notched circular tubes under cyclic bending," *J. Mech.*, vol. 26, no. 3, 2010, pp. 403-411.
  - [14] K.-L. Lee, "Mechanical behavior and buckling failure of sharp-notched circular tubes under cyclic bending," *Struct. Eng. Mech.*, vol. 34, no. 3, 2010, pp. 367-376.
  - [15] K.-L. Lee, C.-M. Hsu, and W.-F. Pan, "Viscoplastic collapse of sharp-notched circular tubes under cyclic bending," *Acta Mech. Solida Sinica*, vol. 26, no. 6, 2013, pp. 629- 641.
  - [16] K.-L. Lee, C.-M. Hsu, and W.-F. Pan, "Response of sharp-notched circular tubes under bending creep and relaxation," *Mech. Eng. J.*, vol. 1, no. 2, 2014, pp. 1-14.
  - [17] C.-C. Chung, K.-L. Lee, and W.-F. Pan, "Collapse of sharp-notched 6061-T6 aluminum alloy tubes under cyclic bending," *Int. J. Struct. Stab. Dyn.*, vol. 16, no. 7, 2016, 1550035 (24 pages).
  - [18] K.-L. Lee, W.-F. Pan, and J.-N. Kuo, "The influence of the diameter-to-thickness ratio on the stability of circular tubes under cyclic bending," *Int. J. Solids Struct.*, vol. 38, no. 14, 2001, pp. 2401-2413.
  - [19] K.-H. Chang, K.-L. Lee, and W.-F. Pan, "Buckling failure of 310 stainless steel tubes with different diameter-to-thickness ratios under cyclic bending," *Steel Comp. Struct.*, vol. 10, no. 3, 2010, pp. 224-245.
  - [20] K.-L. Lee, C.-M. Hsu, and W.-F. Pan, "The influence of the diameter-to-thickness ratio on the response and collapse of sharp-notched circular tubes under cyclic bending," *J. Mech.*, vol. 28, no. 3, 2012, pp. 461-468.

## AUTHORS' PROFILES



**Kuo-Long Lee** received the Ph.D. degree in Dept. of Engineering Science from National Cheng Kung University in Taiwan in 2000. Currently working as Prof. in Dept. of Innovative Design and Entrepreneurship from Far East University in Taiwan.



**Wen-Fung Pan** received the Ph.D. degree in Dept. of Civil and Environmental Engineering from University of Iowa in USA in 1989. Currently working as Prof. in Dept. of Engineering Science from National Cheng Kung University in Taiwan.